Computational Model of Coils for Wireless Power Transfer with Reluctance Network Analysis

Keita Furukawa
Nagaoka University of Technology
Nagaoka-city, Japan
archer_FK@stn.nagaokaut.ac.jp

Keisuke Kusaka
Nagaoka University of Technology
Nagaoka-city, Japan
kusaka@vos.nagaokaut.ac.jp

Jun-ichi Itoh
Nagaoka University of Technology
Nagaoka-city, Japan
itoh@vos.nagaokaut.ac.jp

***Abstract*— This paper proposes an analytical model of the coils in wireless power transfer systems for electric vehicles with reluctance network analysis (RNA) in order to shorten a design process of the coils. A transmitting coil and a receiving coil are modeled with magnetomotive force and numerous hollow-cylindrical units of a magnetic circuit. Circular coils with ferrite plates are modeled with RNA to demonstrate the validity of a RNA model. The values of the mutual inductance between the transmitting coil and the receiving coil are compared between the prototype and the RNA model with changing a radius of the windings and an air gap from the transmitting coil to the receiving coil. As a result, the error of the values of the mutual inductance between the prototype and the RNA model is less than 20% when the radius of the windings is from 40 to 80 mm, and when the air gap between the coils is from 30 to 150 mm. The RNA model is able to calculate the mutual inductance in a short time.**

Keywords—wireless power transfer, coil, magnetic circuit, reluctance network analysis

I. INTRODUCTION

Wireless power transfer systems have been actively studied for battery charging systems of electric vehicles to avoid electric shocks for more safety [1–3]. In particular, inductive power transfer (IPT), which transmits power with magnetic coupling between transmitting coils and receiving coils, is attracted to the battery charging systems in order to achieve high power and high system efficiency. Maximum efficiency and a maximum power of IPT systems depend on the quality factor and the coupling factor of IPT coils [3]. Thus, designing IPT coils is one of the essential processes of the IPT-system design [1–3].

Self-inductance and mutual inductance of the transmitting coil and the receiving coils are generally designed with simulations or prototypes in the design process [4–5]. Both the simulation such as the finite element method (FEM) and the test on numerous prototypes are basically trial-and-error methods, which are time-consuming.

Models using reluctance network analysis (RNA) are proposed for the analysis of inductors or motors to shorten the design process [6–11]. RNA expresses the inductors or the motors into a magnetic circuit made of numerous reluctances and magnetomotive force [6–11]. RNA models are useful in the design process because it is simple to design both the shape and the size of the inductors or the motors in the first design step in exchange for low accuracy [8–11]. However, RNA has not been used for the design processes of the coils for IPT systems since models of the IPT coils require accurate distribution of magnetic flux. An advantage of RNA is expressable of the overall distribution of the magnetic flux in a short time. However, it is impossible to assign the materials being smaller than the unit of the magnetic circuit, which means that calculating the self-inductance is impossible with only RNA in accuracy. Whereas, FEM is able to calculate distribution of magnetic flux in detail. However, FEM need a long time to calculate.

This paper proposes the modeling method of the IPT coils with RNA to shorten the design process of the mutual inductance. The originality of this paper is the proposal of the modeling method with RNA, transformation of cores, and a circuit simulator. The time-consuming in the conventional design processes of the IPT coils is that the mutual inductance is calculated with FEM at numerous conditions. The self-inductance and the mutual inductance are designed with separate processes because the variation of the self-inductance is generally less influenced by the air-gap and position misalignment. Thus, time of the overall design process expects to be short when the self-inductance and the mutual inductance are calculated with FEM and RNA, respectively. A prototype of circular IPT coils is expressed with RNA as an electric network circuit using magnetomotive force and hollow-cylindrical units of a magnetic circuit. In addition, the calculated mutual inductance with the RNA model between the transmitting coil and the receiving coil is compared with the prototype of the circular IPT coils.

II. RELUCTANCE NETWORK ANALYSIS

A. Structure of Circular Coils for IPT System

Figure 1 shows the structure of the circular coils without coil misalignment. Although various forms of the coils are proposed from the viewpoints of robustness for misalignment, cost and leakage magnetic flux of the IPT systems, the simple circular IPT coils are widely employed [1]. The ferrite plates are placed on the outer side of the pair of the windings in order to decrease reluctance of the coils and leakage magnetic field around the IPT coils.

The IPT systems have much leakage magnetic flux due to the wide-gap coils for in comparison with that of motors or

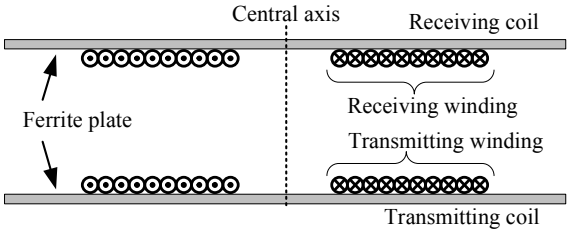

Fig. 1. Sectional view of circular coils for IPT systems.

978-1-7281-5067-3/19/$31.00 ©2019 IEEE

inductances because of high ratio of non-magnetic materials to magnetic materials in the magnetic path. In addition, the magnetomotive force generated by the coils should be also considered because the shape of the coils influences the magnetic flux distribution. Thus, a model of the coils requires to express the three-dimensional distribution of the magnetic flux in detail. RNA is able to express the distribution of the magnetic flux. In the next section, an outline of RNA is explained.

B. Outline of RNA

Reluctance network analysis is one of permeance methods using ideas that models are constructed with numberless small units. RNA expresses the IPT coils including air around the coils as a magnetic circuit with and numerous units of magnetic circuit. In addition, magnetomotive force generated by windings is also set onto the units of magnetic circuit. The reluctances are assigned into the units of magnetic circuit with considering the three-dimensional magnetic flux. The distribution of magnetic flux in the constructed RNA model is calculated with circuit simulators as an electric network. Finally, magnetic characteristics such as values of the mutual inductance between the transmitting coil and the receiving coil are obtained from the calculation.

The advantage of RNA is shorter computing time than FEM [9–10]. In the previous studies, a computing time of a proposed model based on RNA is ten or more times faster than computing times of FEM models [9–10]. In addition, waveforms of magnetic flux density calculated with RNA models almost correspond to waveforms of FEM models or motors [8–11]. Thus, the RNA model of the IPT coils is expected to estimate the values of the mutual inductance which require the accurate interlinkage magnetic flux.

C. Unit of Magnetic Circuit for Analysis of IPT Coils

Figure 2 shows the hollow-cylindrical unit of the magnetic circuit. The RNA model of IPT coils is filled with the unit of the magnetic circuit in Fig. 2. The RNA model is considered under the cylindrical coordinate system because the circular coils such as Fig. 1 is axial symmetry. The θ-axis reluctances in the unit are unnecessary to consider because θ-axis magnetic flux generated by the circular coil is zero. The reluctances R_{re}, R_{ri}, R_{zt}, and R_{zu} in the cylindrical unit of Fig. 2 are calculated from the size of the unit, and expresses as

$$R_{re} = \int_{r-\frac{\Delta r}{2}}^{r} \frac{1}{2\pi\mu r \Delta d} dr = \frac{1}{2\pi\mu\Delta d} \ln\left(\frac{2r}{2r-\Delta r}\right) \quad \text{..... (1),}$$

$$R_{ri} = \int_{r-\Delta r}^{r-\frac{\Delta r}{2}} \frac{1}{2\pi\mu r \Delta d} dr = \frac{1}{2\pi\mu\Delta d} \ln\left\{\frac{2r-\Delta r}{2(r-\Delta r)}\right\} \quad \text{..... (2),}$$

$$R_{zt} = R_{zu} = \frac{\Delta d}{2\pi\mu(2r-\Delta r)\Delta r} \quad \text{.....(3),}$$

where Δd is the height, Δr is the increment of the radius, r is the external radius and μ is the magnetic permeability of the materials, e.g., air and ferrite. Note that the magnetic flux through R_{re}, R_{ri}, R_{zt}, and R_{zu} are integrated value on the side surfaces, the upper surface or the undersurface of the unit of the magnetic circuit.

D. Magnetomotive Force

Figure 3 shows a part of the RNA model including the windings in which the current I flows. In general, Gauss' law for magnetism and Ampere's circuital law in a magnetic circuit can be applied similarly to Kirchhoff's current law and voltage law for an electrical circuit, respectively [11–12]. When an arbitrary closed-loop c is defined in the magnetic circuit, Ampere's circuital law is also adapted to c to estimate a closed curve. The magnetomotive force F_c of c is shown as

$$F_c = \sum_n R_n \phi_n = \oint_c \boldsymbol{H}_c \bullet d\boldsymbol{r} = \int_S \boldsymbol{j}_c \bullet d\boldsymbol{S} \quad \text{..... (4),}$$

where R_n is one of reluctances on c, ϕ_n is the magnetic flux through R_n, $\boldsymbol{H}_c$ is the magnetic field at a certain point on c, and $\boldsymbol{j}_c$ is the current density inside the closed surface S.

When (4) is adapted to the closed-loops c_1, c_2, and c_3 in Fig. 3 (a) as examples, the magnetomotive force F_{c1}, F_{c2} and F_{c3} of each closed-loop are expressed as

$$F_{c1} = 0 \quad \text{..... (5),}$$

$$F_{c2} = I \quad \text{..... (6),}$$

$$F_{c3} = I - I = 0 \quad \text{..... (7).}$$

The magnetomotive force is applied onto all units of the magnetic circuit inside the coils with the value of I to fulfill (5–7). When there are plural windings in the RNA model, the magnetomotive force is set the overall closed surface of each winding with the value of flowing current from the principle of superposition. Moreover, the interlinkage flux is the sum of the magnetic flux through the magnetomotive force of each winding.

III. Prototype of Circular IPT Coils

A. Prototype of Circular IPT Coils

Figure 4 shows the prototype of the circular IPT coils. The prototype is constructed by a pair of facing coils: the transmitting coil in Fig. 4 (a) and the receiving coil in

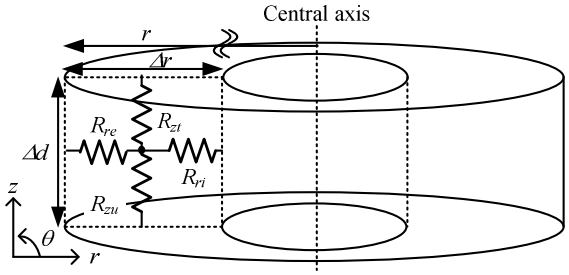

Fig. 2. Unit of magnetic circuit in RNA model.

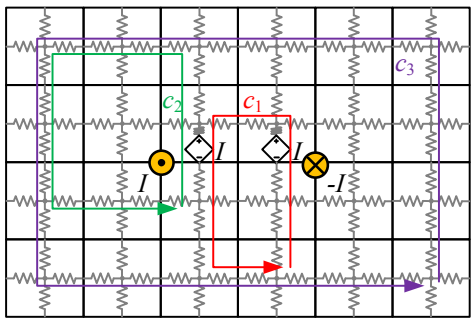

Fig. 3. Distribution of magnetomotive force in RNA model.

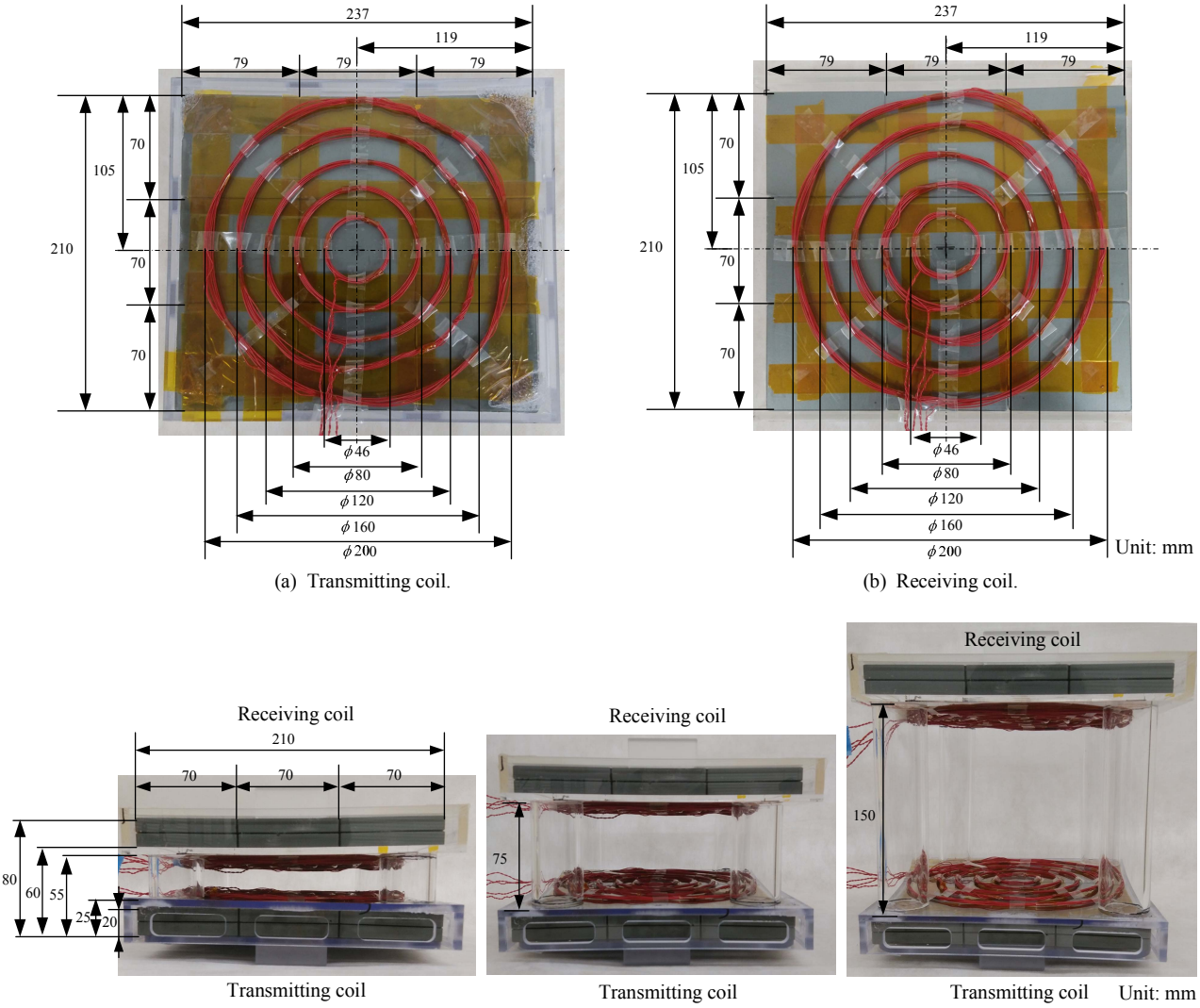

(a) Transmitting coil. (b) Receiving coil.

(c) Side view with 30-mm gap. (d) Side view with 75-mm gap. (e) Side view with 30-mm gap.

Fig. 4. Prototype of circular IPT coil.

Fig. 4 (b). The transmitting coil and the receiving coil are the same forms, material, and size for simplification.

The ferrite plates of the transmitting coil and the receiving coil is a length of 237 mm, a width of 210 mm, and a height of 20 mm. The ferrite plate is constructed by 18 smaller square ferrite plates whose domain is a length of 79 mm, a width of 70mm, and a height of 10 mm. The magnetic material of the ferrite plate is PC40 (TDK). Moreover, the ferrite plate is covered with the acrylic case whose thickness is 5 mm.

Wires with a cross-section of 0.126 mm^2 is used for each circular winding in Fig. 4 (a) and Fig. 4 (b). The number of the winding N is 10. The radiuses of the five circular windings are 23, 40, 60, 80 and 100 mm, respectively. The five circular windings have a role of changing the radius of the windings r_{ce} when the prototype is compared with a proposed RNA model. Note that unwanted windings are open in order to ignore themselves when measuring the values of the mutual inductance because the magnetomotive force generated by the open windings is zero.

Figures 4 (c-e) show the side view of the prototype with changing the gap h_g between the transmitting coil and the receiving coil. The gap is changed from 30 mm to 150 mm to evaluate the effect of the air-gap on the mutual inductance.

B. Conversion from Square Ferrite Plate to Circular Ferrite Plate

Chapter II shows the RNA model of the axisymetric IPT coils. However, the prototype is not directly translated to an RNA model because the square ferrite plates of the prototype are not suitable for an axisymetric RNA model. Thus the form of the ferrite plates should be changed to a cylinder which has the same values of the mutual inductance, to express the prototype as the RNA model. Thus, a radius r_{fe} of the ferrite plates whose characteristic of the mutual inductance is the same as the prototype, is clarified with four FEM models.

The FEM models are built on JMAG (JSOL). JMAG is one of electromagnetic-field-analysis software with the FEM. The value of r_{fe} is determined to be the lowest relative error of the mutual inductance in the FEM models by comparing the value of the mutual inductance between the FEM models and the prototype.

Figure 5 shows the rotary surface of the FEM models and the top view of ferrite plates on FEM models. The FEM models are

I. FEM model of the prototype whose size and form are as same as the prototype,
II. Narrow-side model whose 105-mm r_{fe} is equal to half width of prototype,
III. Average-core-length model whose 132-mm r_{fe} is equal to the average of half width and half diagonal of prototype, and
IV. Diagonal model whose 158-mm r_{fe} is equal to half diagonal of prototype.

Note that the depths of the circular ferrite plates and the acrylic cases in the FEM models are 20 and 5 mm as same as the prototype in Fig. 4, respectively. In addition, the height and width of the windings in the FEM models are 3 mm referred to an approximate value of the prototype.

Figure 6 shows the relative error $\Delta M / M_m$ of the mutual inductance of the four FEM models when r_{ce} and h_g are changed. The true values of the mutual inductance in Fig. 6 are measured values of the mutual inductance M_m of the prototype under the same conditions. Figure 6 (a–c) show $\Delta M / M_m$ with h_g = 30 mm, h_g = 75 mm, and h_g = 150 mm, respectively. The relative error $\Delta M / M_m$ of the the FEM model of prototype comes from the dimension error and the measurement error of the mutual inductance on the prototype.

Figure 6 shows that $\Delta M / M_m$ of Average-core-length model are small. In addition, fluctuation of $\Delta M / M_m$ of the average-core-length model is the same as the fluctuation of FEM model of the prototype. Whereas, $\Delta M / M_m$ of Narrow-side model and Diagonal model are large when r_{ce} is increased. It indicates that the effect of the magnetic flux near the edge of the ferrite plates is not negligible when r_{ce} is close to r_{fe}. The reason why $\Delta M / M_m$ at r_{ce} = 23 mm is large in all of FEM models, is deduced from the dimension error and the measurement error of the prototype. It is difficult to measure inductance lower than μH-order.

As a result, the RNA model should be built based on the average-core-length model. Therefore, r_{fe} of the circular ferrite plates in the RNA model is 132 mm.

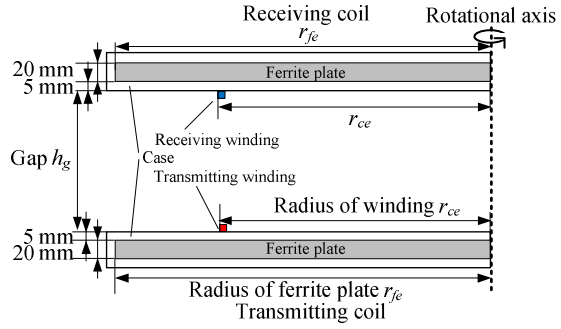

(a) Rotary surface of circular model.

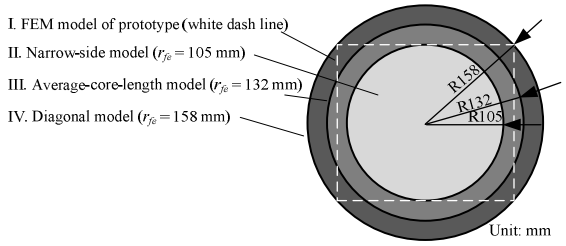

(b) Top view of ferrite plates of each FEM model.

Fig. 5. Configuration of FEM models

IV. RNA Model of Prptotype

Figure 7 shows the RNA model employed with the IPT coils in Fig. 4. The RNA model is used by 195 units. The numbers of the units to the r-axis and the z-axis are 13 and 15, respectively. The white units express air domain (the relative permeability is one). The units colored by grey express ferrite-plate domain (the relative permeability is 2300).

The air space around the coils including the air gap is also considered because the magnetic flux through the air space affects calculated values of the mutual inductance. The length of the r-axis is 232 mm. The length of the z-axis is from 170 mm to 290 mm depending on h_g. In addition, the dimensions of each unit Δd and Δr are determined to be lower than 30 mm. The height Δd of the units expressing the ferrite plates

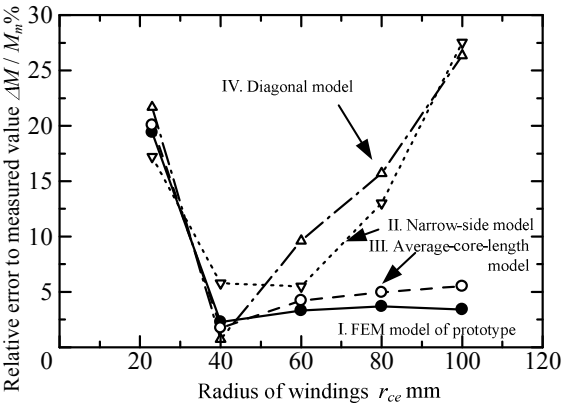

(a) h_g = 30 mm.

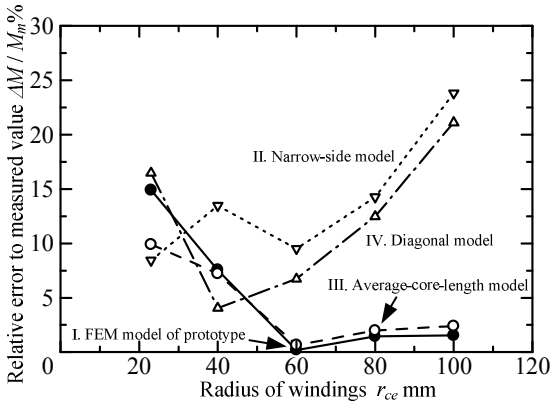

(b) h_g = 75 mm.

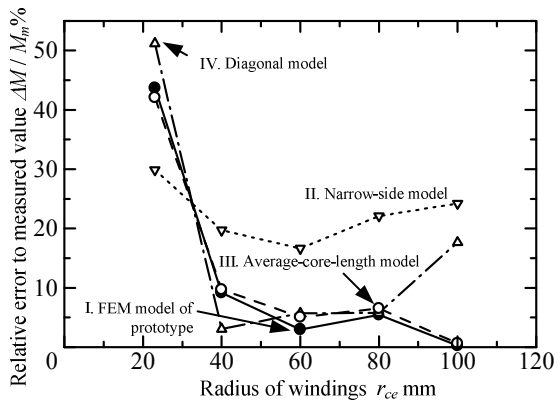

(c) h_g = 150 mm.

Fig. 6. Relative error of mutual inductance.

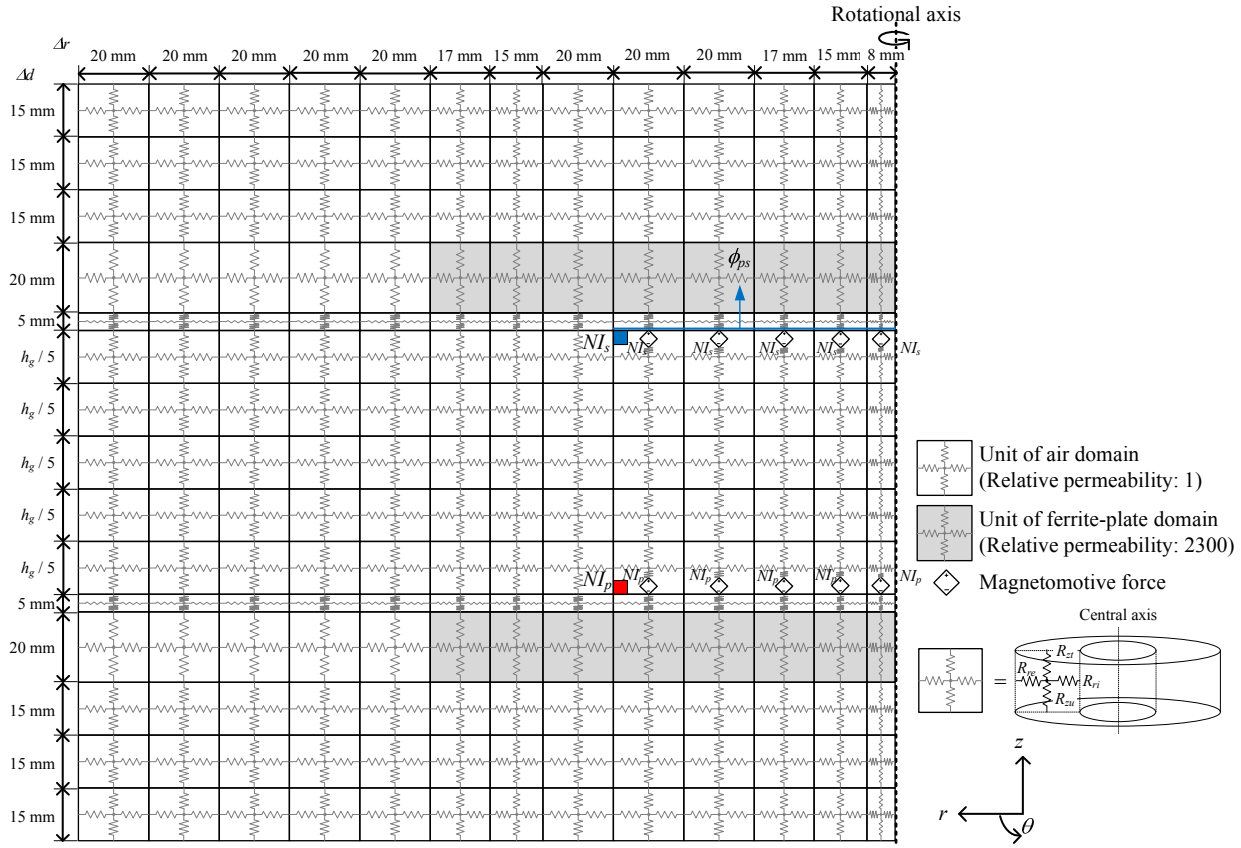

Fig. 7. Representative example of RNA model (Radius r_{ce} of windings is 80 mm).

and the air domain aligned horizontally to the ferrite plates is 20 mm. The increment Δr of the units expressing the ferrite plates and the air domain aligned vertically to the ferrite plates are decided to meet the external diameter of the units and windings of the prototype in Fig. 4. Note that Δr of the units next to the central axis is 8 mm to reduce the modeling error. A 5-mm thickness of the acrylic cases between the ferrite plates and the windings is also considered with the units of the air domain. The terminals on the boundary of the RNA model is opened. The magnetomotive forces NI_p and NI_s of the transmitting coil and the receiving coil are located inside the units of each winding.

V. Comparison of Mutual Inductance

In this chapter, the RNA model in Fig. 7 are compared with the prototype in term of the mutual inductance between the transmitting coil and receiving coil. The RNA model is modeled and calculated with PLECS (Plexim). The mutual inductance between the transmitting coil and the receiving coil is compared with changing r_{ce} and h_g.

In addition, a criterion of the RNA model is shown as a reference in order to confirm the validity of the RNA model; The RNA model is available in a design process of the circular IPT coils when the error of the mutual inductance between the RNA model and the prototype is less than 20%. A error of 20% on the mutual inductance is decided from experiencing things that there is a possibility to become errors of inductance between real IPT coils and FEM models to 20%.

Figure 8 shows the mutual inductance against r_{ce} and h_g with the RNA model and the prototype. The black circles with the full-line is the results with the proposed model of RNA, whereas the white-painted plots with dashed line indicates the results with the prototype. The mutual inductances are calculated from the interlinkage magnetic flux ϕ_{ps} of the receiving winding and I_p when the receiving winding is open (I_s = 0). The x-axis is the ratio r_{ce} / r_{fe} of the radius of the windings standardized by r_{fe} = 132 mm, whose value is decided in Chapter III. Note that the maximum value of r_{ce} / r_{fe} is 0.795 because r_{ce} is limited by the width of the ferrite plates from construction of the IPT coils.

The values of the mutual inductance of the RNA model is the same as the value of the mutual inductance of the prototype in the order of magnitude at same r_{ce} and h_g. The result means that RNA is employed to the simplified design of the circular IPT coils. In addition, the errors of the mutual inductance are less than 20% in the range of as follows: the ranges of r_{ce} / r_{fe} is from 0.30 to 0.76 when h_g is 30 or 75 mm. The ranges of r_{ce} / r_{fe} is from 0.30 to 0.61 when h_g is 150 mm.

The error of the mutual inductance are larger than 20% at r_{ce} / r_{fe} = 0.17 because of the dimension error and the measurement error of the prototype. However, the error of the mutual inductance is larger than 20% at r_{ce} / r_{fe} = 0.76 and h_g = 150 mm. Factors of the large error are neither the dimension error nor the measurement error of the prototype because the relative error of the mutual inductance with Average-core-length model in Fig. 6 (c) is 1%. Thus, the RNA model does not express the distribution of magnetic flux completely. As supposition, the unit of the magnetic circuit in Fig. 2 does not consider reluctances of the diagonal path. The measured mutual inductance of the prototype is more increasing due to spreading lines of magnetic force around the IPT coils when r_{ce} and h_g are large.

Although it is impossible to calculate the self-inductance with only the RNA model in the chapter 1 in accuracy, the maximum relative error of the self-inductance is 27.8% under the conditions of $r_{ce} / r_{fe} = 0.30$, $h_g / r_{fe} = 1.14$ and 3-mm height and width of the windings. The order of magnitude of the self-inductance is able to estimate with the RNA model.

Moreover, the computation time under the all conditions with the RNA model is 20 second, which is shorter than 3676 second with 3-D FEM models of the prototype.

As a conclusion, the RNA model is available to the design process of the circular IPT coils when the ratio r_{ce} / r_{fe} are from 0.30 to 0.61, and when the ratio h_g / r_{fe} are from 0.23 to 1.14. Moreover, the RNA model contributes to shorten the design process of the IPT coils.

VI. Conclusions

This paper examines the RNA model into the design progress of the circular coils in IPT systems to shorten the design process. The RNA model would be applied at the first step of the design progress to reduce the number of trials conducting by the conventional time-consuming design method such as simulations with FEM or the construction of numerous prototypes. The RNA model is simply constructed by numerous hollow-cylindrical units of the magnetic circuit and the magnetomotive force. In order to verify the validity of the RNA model, the mutual inductances of the transmitting coil and the receiving coil are compared with the RNA model and the prototype of the circular IPT coils. As a result, the mutual inductance agreed with lower than 20% error in the range of the radius and the gap of the windings from 40 mm to 80 mm and 30 mm to 150 mm, respectively. In addition, the relation of the mutual inductance is matched in the overall range of the radius and gap of the windings. Thus, the model of RNA was suitable to simplify the design progress of the coils in IPT systems.

In the future, the accuracy of the RNA model will be improved in term of mutual inductance and self-inductance.

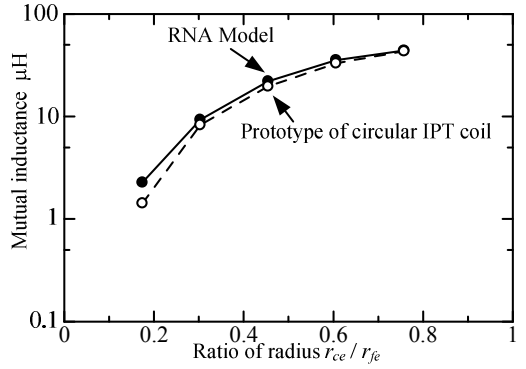

(a) $h_g = 30$ mm ($h_g / r_{fe} = 0.23$).

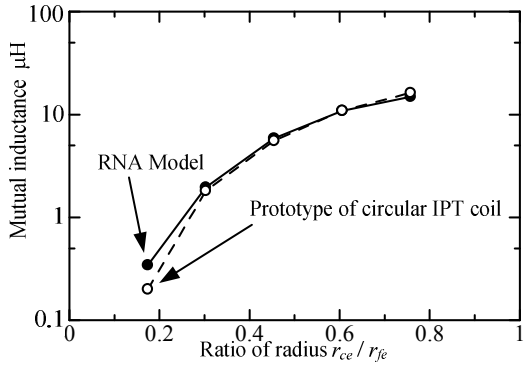

(b) $h_g = 75$ mm ($h_g / r_{fe} = 0.57$).

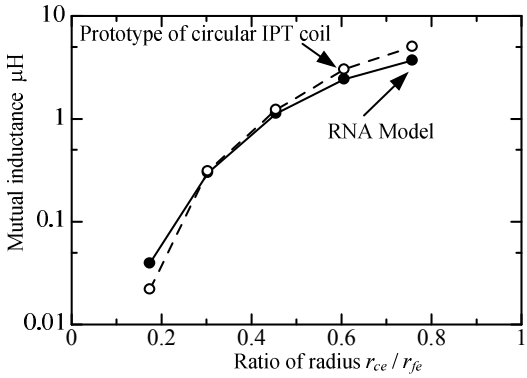

(c) $h_g = 150$ mm ($h_g / r_{fe} = 1.14$).

Fig. 8. Mutual inductance of prototype and RNA model.

References

[1] D. Patil, M. K. McDonough, J. M. Miller, B. Fahimi and P. T. Balsara, "Wireless Power Transfer for Vehicular Applications: Overview and Challenges", IEEE Transactions on Transportation Electrification, Vol. 4, No. 1, pp. 3-37 (2018)

[2] K. Kusaka and J. Itoh: "Development Trends of Inductive Power Transfer Systems Utilizing Electromagnetic Induction with Focus on Transmission Frequency and Transmission Power", IEEJ Journal of Industry Applications, Vol. 137, No. 5, pp. 328-339 (2017)

[3] S. Li, and C. C. Mi: "Wireless Power Transfer for Electric Vehicle Applications", IEEE Journal of Emerging and Selected Topics in Power Electronics, Vol. 3, No. 1, pp. 4-17 (2015)

[4] R. Bosshard and J. W. Kolar: "Multi-Objective Optimization of 50 kW/85 kHz IPT System for Public Transport", IEEE Journal of Emerging and Selected Topics in Power Electronics, Vol. 4, No. 4, pp. 1370-1382 (2016)

[5] H. Kim, C. Song, Dong-Hyun Kim, D. H. Jung, In-Myoung Kim, Young-Il Kim, J. Kim and S. Ahn: "Coil Design and Measurements of Automotive Magnetic Resonant Wireless Charging System for High-Efficiency and Low Magnetic Field Leakage", IEEE Transactions on Microwave Theory and Techniques, Vol. 64, No. 2, pp. 383-400 (2016)

[6] J. Cale, S. D. Sudhoff and Li-Quan Tan: "Accurately Modeling EI Core Inductors Using a High-Fidelity Magnetic Equivalent Circuit Approach", IEEE Transactions on Magnetics, Vol. 42, No. 1, pp. 40-46 (2006)

[7] J. Brudny, G. Parent, and I. Naceur: "Characterization and Modeling of a Virtual Air Gap by Means of a Reluctance Network", IEEE Transactions on Magnetics, Vol. 53, No. 7, pp. 1-7 (2017)

[8] Y. Yoshida, K. Nakamura, O. Ichinokura, and Katsubumi Tajima: " Efficiency Optimization of SPM Motor Considering Carrier Harmonics Based on Electric and Magnetic Networks", IEEJ Journal of Industry Applications, Vol. 3, No. 6, pp. 422-427 (2014)

[9] Y. Yoshida, K. Nakamura, and O. Ichinokura: "Evaluation of Influence of Carrier Harmonics of SPM Motor Based on Reluctance Network Analysis", IEEJ Journal of Industry Applications, Vol. 3, No. 4, pp. 304-309 (2014)

[10] S. Bazhar, J. Fontchastagner, N. Takorabet, and N. Labbe: "Hybrid Analytical Model Coupling Laplace's Equation and Reluctance Network for Electrical Machines", IEEE Transactions on Magnetics, Vol. 53, No. 6, pp. 1-4 (2017)

[11] H. Xie, G. Krebs, M. H. Hassan, M. Zhang and C. Marchand: "A New Reluctance Network-Based Method With Complementary Distributed Magnetomotive Forces", IEEE Transactions on Magnetics, Vol. 55, No. 6, pp. 1-5 (2019)

[12] H. C. Roters: "ELECTROMAGNETIC DEVICES FIRST EDITION", New York JOHN WILEY & SONS, Inc. (1941)